Optics Letters

Analysis of non-linearity in differential wavefront sensing technique

HUI-ZONG DUAN, YU-RONG LIANG, AND HSIEN-CHI YEH*

MOE Key Laboratory of Fundamental Physical Quantities Measurement, School of Physics, Huazhong University of Science and Technology, 1037 Luo Yu Road, Wuhan 430074, China
**Corresponding author: yexianji@mail.hust.edu.cn*

Received 21 October 2015; revised 11 December 2015; accepted 27 January 2016; posted 28 January 2016 (Doc. ID 251544); published 19 February 2016

An analytical model of a differential wavefront sensing (DWS) technique based on Gaussian Beam propagation has been derived. Compared with the result of the interference signals detected by quadrant photodiode, which is calculated by using the numerical method, the analytical model has been verified. Both the analytical model and numerical simulation show milli-radians level non-linearity effect of DWS detection. In addition, the beam clipping has strong influence on the non-linearity of DWS. The larger the beam clipping is, the smaller the non-linearity is. However, the beam walking effect hardly has influence on DWS. Thus, it can be ignored in laser interferometer.

OCIS codes: (260.0260) Physical optics; (260.3160) Interference; (200.1130) Algebraic optical processing.

http://dx.doi.org/10.1364/OL.41.000914

Optical interferometers have significant applications in the field of high-precision metrology, in which displacements are measured in nano- or pico-meter level. The benefit from using the differential wavefront sensing (DWS) technique is that people can make interferometers measure both the translation and rotation of the target mirror. In many space borne science missions, such GRACE Follow-On [1], LISA Pathfinder[2], SAGM [3], and TianQin [4], laser interferometers are used to determine the variation of distance between proof masses, the altitude jitter of the satellites, and the rotation of the proof mass inside the gravitational reference sensor in pico-meter and nano-radian precision.

In DWS technique, the angle made by two interfering beam axes is related to phase differences between different quadrants of the quadrant photo diode (QPD). The high sensitivity and great common-mode rejection make it a good choice for precision angle measurement. To date, a lot of theoretical and experimental work has been done on optical interfering measurement, including translation phase readout with single element photo diode and rotational phase difference readout with DWS technique. In 2010, Hechenblaikner [5] built an analytical model of DWS detection. However, in their analytical model the beam walking and beam clipping are ignored. The Albert Einstein Institute (AEI) research group did a series of studies on modeling and simulating the optical signals output by laser interferometer. Based on a TEM00 Gaussian beam model, they built a simulating method for the readout of lengths and angles in laser interferometers [6]. They analyzed tilt-to-path length coupling [7], beam clipping effect [8], and general astigmatic Gaussian beams [9]. In order to design and simulate laser interferometer optical system, they developed a computer-aid design software of C++ programming language named IfoCAD.

Based on all the work mentioned above, we derived an analytical expression of DWS detection to explain the non-linearity effect in DWS detection, and also to discuss the influence of beam walking and beam clipping effects. Beam walking means the laser beam rotates around a point that is not located on the QPD surface. Based on the analytical expression we have derived in this paper, the non-linearity property of the DWS has been studied. The results provide us a physical insight into the differential wavefront detection.

The propagation of laser beams in free space is governed by Maxwell's equations, and the Gaussian beam model is the most fundamental solution under paraxial approximation. Thus we can use parameters, phase Φ and amplitude A, to describe a laser beam:

$$E(r_b, z_b, t) = A(r_b, z_b)\exp[i2\pi f t - i\Phi(r_b, z_b)]. \quad (1)$$

In the expression above, (r_b, z_b) represents the cylinder coordinate and f represents laser frequency. Subscript b represents this formula written in the beam coordinate system, whose origin is located at the beam waist. In Eq. (1), the beam amplitude and phase distribution are

$$A(r_b, z_b) = \sqrt{\frac{2P}{\pi\omega^2(z_b)}}\exp\left[-\frac{r_b^2}{\omega^2(z_b)}\right], \quad (2)$$

$$\Phi(r_b, z_b) = \frac{kr_b^2}{2R(z_b)} - \eta(z_b) + kz_b. \quad (3)$$

In these equations, $k = \frac{2\pi}{\lambda}$ represents the wave number of the laser beam, P represents the laser power, η is the Gouy phase, and ω_0 is the beam waist radius.

In the simplest case, where two laser beams interfere on the square quadrant photo diode as shown in Fig. 1, the interference term output by the QPD sensor can be written as

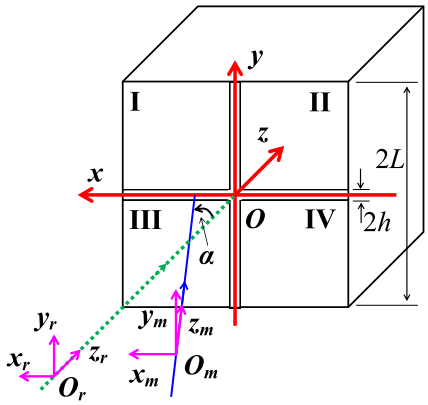

Fig. 1. Coordinate system in laser interferometer, which two laser beams interfere on the surface of a square QPD: L is half-edge length of the QPD; h is half-width of gap between different quadrants; α is incident angle of measurement beam; and O_m and O_r are the origins of measurement and reference beam coordinates.

S表示微元面积

$$P_S = \int_S \mathrm{d}S|E_m + E_r|^2. \tag{4}$$

In Eq. (4), S represents a finite sensing area of the QPD, and P_S is the power as it impinges on a surface S. In this optical system, the two beams act as a reference beam and measurement beam, whose beam axes are plotted in dashed lines and bold lines as shown in Fig. 1. By substituting Eq. (1) into Eq. (4), we can derive the expression of the beat note signal:

$$P_{AC} = \frac{1}{(P_m + P_r)} \frac{\sqrt{P_m P_r}}{\pi \omega_m \omega_r} \int_S \mathrm{d}S \times \exp\left(-\frac{r_m^2}{\omega_m^2} - \frac{r_r^2}{\omega_r^2}\right) \cos[2\pi \Delta f t - \Delta\Phi]. \tag{5}$$

In Eq. (5), subscript m and r represent the measurement and reference beams, $P_{m,r}$ are the laser power, $\omega_{m,r}$ are the beam spot radius, $\Delta f = |f_m - f_r|$ is the beat frequency, and $\Delta\Phi = \Phi_m - \Phi_r$ is the phase difference between two incident beams. In practice, the laser beams are misaligned and mismatched. In order to describe the tilt and shift of the laser beams, we introduce a coordinate transformation. Let the QPD detecting surface be located at $z = 0$. Any point on the detecting surface is written as $\vec{r} = (x, y, 0)^T$. Let the initial intersection points of laser beam axes with the detecting surface be $\vec{r}^{\,i}_{m,r} = (x_i, y_i, 0)^T_{m,r}$. Assuming that the beams are rotated around a pivot $\vec{r}^{\,p}_{m,r} = (x_p, y_p, z_p)^T_{m,r}$ and a fixed normalized vector $\vec{e}_{m,r} = (n_x, n_y, n_z)^T_{m,r}$. Thus, the transformation between the beam coordinates and the detecting coordinate can be formulated by

$$\vec{r}^{\,b}_{m,r} = M^{-1}_{m,r}[\vec{r} - \vec{r}^{\,p}_{m,r}] + \vec{r}^{\,p}_{m,r} - \vec{r}^{\,i}_{m,r}. \tag{6}$$

In Eq. (6), $M_{m,r}$ is the Rodrigues' matrix in 3D Cartesian coordinate, which can describe any rotation in 3D linear space. Substituting the coordinate transformation into Eq. (5), and assuming that during the movement the radius of beam spots on photo diode $\omega_{m,r}$, Gouy phases of beams $\eta_{m,r}$, and wavefront radius $R_{m,r}$ remain the same, means these parameters are z dependent. After that we can get the expression of the integrand in Eq. (5):

$$\begin{aligned} I &= \exp\left(-\frac{r_m^2}{\omega_m^2} - \frac{r_r^2}{\omega_r^2}\right) \cos[2\pi \Delta f t - \Delta\Phi] \\ &= \exp[-(A_1 x^2 + A_2 xy + A_3 x + A_4 y^2 + A_5 y + A_6)] \\ &\quad \times \cos[B_1 x^2 + B_2 xy + B_3 x + B_4 y^2 + B_5 y + B_6]. \end{aligned} \tag{7}$$

As the heterodyne frequency term will be canceled in the data processing of the phase meter unit, we assume constant laser frequencies here. Rewriting Eq. (7) in exponential form by extending the integrand into the complex domain, we can get

$$I^c = \exp\left[-\begin{pmatrix} x \\ y \\ 1 \end{pmatrix}^T \begin{pmatrix} C_1 & C_2 & C_3 \\ 0 & C_4 & C_5 \\ 0 & 0 & C_6 \end{pmatrix} \begin{pmatrix} x \\ y \\ 1 \end{pmatrix}\right]. \tag{8}$$

In the formula above, $C_k = A_k - iB_k$, $k = 1, 2, \ldots, 6$, Eqs. (5) and (8) govern the output signals of the interferometer. All the equations above are cited from Ref. [8].

We calculate the DWS signal for a simple case that the reference beam impinges normally at the center of the QPD, and measurement beam rotates around the pivot $\vec{r}^{\,p}_m = (0, 0, -z_p)^T$ and the y-axis $\vec{e}_m = (0, 1, 0)^T$, $\alpha_m = \alpha$, which is shown in Fig. 1. In this case, all the parameters are listed in Table 1.

Substituting all the parameters in Table 1 into Eq. (8) and calculating Eq. (5) for the left and right half-domains of the quadrant photo detector, we can get the interfering signals as shown in the following equations:

$$I_{L,R} = C_0 \int_{\Gamma_x^{L,R}} \exp\left[-C_1\left(x + \frac{C_3}{2C_1}\right)^2\right] \mathrm{d}x \int_{\Gamma_y^{L,R}} \exp(-C_4 y^2) \mathrm{d}y. \tag{9}$$

In Eq. (9), the subscript L and R represent the left and right parts of the detecting surface of the QPD, Γ_L:$x, y \in [-L, -h] \times [-L, L]$ and Γ_R:$x, y \in [h, L] \times [-L, L]$, and $C_0 = \frac{\sqrt{P_m P_r}}{\pi \omega_m \omega_r (P_m + P_r)} \exp(-C_6 + \frac{C_3^2}{4C_1})$. Based on the definition of Gaussian error function in a complex domain, we can get the analytical expression of Eq. (9):

Table 1. Parameters in Intergrand Eq. (8) in a Simple Case [8]

Parameters	Formula Expressions
A_1	$\frac{\cos^2\alpha}{\omega_m^2} + \frac{1}{\omega_r^2}$
A_2	0
A_3	$-\frac{z_p \sin(2\alpha)}{\omega_m^2}$
A_4	$\frac{1}{\omega_m^2} + \frac{1}{\omega_r^2}$
A_5	0
A_6	$\frac{z_p^2 \sin^2\alpha}{\omega_m^2}$
B_1	$-\frac{k_m \cos^2\alpha}{2R_m} + \frac{k_r}{2R_r}$
B_2	0
B_3	$-k_m \sin\alpha + \frac{k_m z_p \sin(2\alpha)}{2R_m}$
B_4	$-\frac{k_m}{2R_m} + \frac{k_r}{2R_r}$
B_5	0
B_6	$-\frac{k_m z_p^2 \sin^2\alpha}{2R_m} + k_m z_p(1 - \cos\alpha)$ $-k_m z_m + k_r z_r - \eta_m + \eta_r$

$$I_L = \frac{\pi C_0}{2\sqrt{C_1 C_4}}\operatorname{erfi}\left(\sqrt{C_4}L\right)\left\{\operatorname{erfi}\left[\sqrt{C_1}\left(-h+\frac{C_3}{2C_1}\right)\right] - \operatorname{erfi}\left[\sqrt{C_1}\left(-L+\frac{C_3}{2C_1}\right)\right]\right\}, \tag{10}$$

$$I_R = \frac{\pi C_0}{2\sqrt{C_1 C_4}}\operatorname{erfi}\left(\sqrt{C_4}L\right)\left\{\operatorname{erfi}\left[\sqrt{C_1}\left(L+\frac{C_3}{2C_1}\right)\right] - \operatorname{erfi}\left[\sqrt{C_1}\left(h+\frac{C_3}{2C_1}\right)\right]\right\}. \tag{11}$$

Finally, the analytical expression for DWS in this simple case can be formulated as follows:

$$\phi_{\text{roty}}^{\text{DWS}} = \arg I_L - \arg I_R. \tag{12}$$

Equation (12) describes the basic physical processing in DWS. In the following, we will discuss the non-linear, beam clipping, and beam walking effects in DWS technique.

Assuming that the incident beams are infinite plane waves, the relative angle α between two beams is small, the slit between the quadrants is negligible, and there is no beam walking effect on the QPD, the DWS response of a square QPD can be written as follows:

$$\phi_{pb}^{\text{DWS}} = \frac{2L\pi}{\lambda}\alpha, \tag{13}$$

where L represents the half-edge length of the QPD, λ is the laser beam wavelength. In Ref. [5], an analytical model of DWS has been derived based on the Gaussian beam model. Without considering the finite QPD surface and beam walking effect, the analytical expression for DWS is formulated as follows:

$$\phi_{\text{inf}}^{\text{DWS}} = \sqrt{\frac{2}{\pi}}\left(k\omega_{\text{eff}}\alpha\left(1-\frac{z_p}{R_{\text{rel}}}\right) - k\frac{\omega_{\text{eff}}x_{0s}}{R_{\text{rel}}}\right)F(\sigma), \tag{14}$$

$$\frac{2}{\omega_{\text{eff}}^2} = \frac{1}{\omega_m^2}+\frac{1}{\omega_r^2}, \qquad \frac{2}{R_{\text{rel}}} = \frac{1}{R_r}-\frac{1}{R_m}, \tag{15}$$

$$F(\sigma) = \frac{1}{\sqrt{2}}\sqrt{\frac{1+\sqrt{1+\sigma^2}}{1+\sigma^2}}, \qquad \sigma = \frac{k\omega_{\text{eff}}^2}{4R_{\text{rel}}}. \tag{16}$$

The three equations listed above are cited from Ref. [5]. Equations (13) and (14) can be used to compare with the analytical expression of Eq. (12), and the comparison result is shown in Fig. 2. In the calculation, we choose two different cases: a QPD with $2h = 10^{-2}$ mm slit, edge length of $2L =$ 20 mm and $2L = 0.5$ mm, respectively. In these two cases, the two beams waist radiuses are 1 mm and both beam waists are located at the center of the QPD surface. Because in the first case QPD surface edge length is three times larger than the beam waist radius, the beam clipping effect can be neglected. In Fig. 2, the dashed line is the result calculated using Eq. (14), and the + plus line is the result calculated using Eq. (12). We can see that the results agree with each other in a small angle. For larger angles, there are some differences between the two results. This is because Eq. (14) is a linearized result. This is similar to the conclusion in Ref [6]. In the second case, we set the beam waist radius much larger than the edge length of QPD. Only a small part near the center of Gaussian beam is detected. Thus we can treat the laser beams as plane beams in this case. In Fig. 2, the bold line is the result calculated using Eq. (13) and the × cross line is the result calculated using

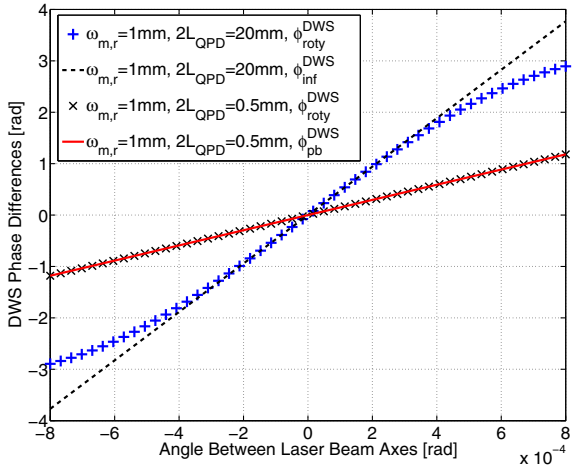

Fig. 2. Comparison of DWS response lines computed with different analytical expressions.

Eq. (12). These two results agree with each other very well. This means that the plane beam approximation is accurate enough to describe the detecting beam in this case.

In the next step, we calculated the DWS response using numerical method and analytical expression. The numerical result is calculated with Optical Simulation, which is a MATLAB function library we developed in 2012. This optical calculation library is similar to IfoCAD, but based on a different developing platform. In the numerical simulation, we first built a computer model of the optical system, which consists of two laser beams and a QPD with square surface, and the phase of heterodyne beat note is calculated numerically based on correlation analysis. The numerical and analytical results matched very well. The residuals after fitting to 1st order are shown in Fig. 3. From the results, we can see the non-linearity of the DWS detection clearly. The magnitude of non-linearity of DWS is a milli-radians level in phase. If we use a linear model to calculate the angle from the detected phase difference, we will have a micro-radians angle detection non-linearity error for milli-radians rotations. In order to analyze this non-linearity effect, we calculated DWS angle measurement response curves under

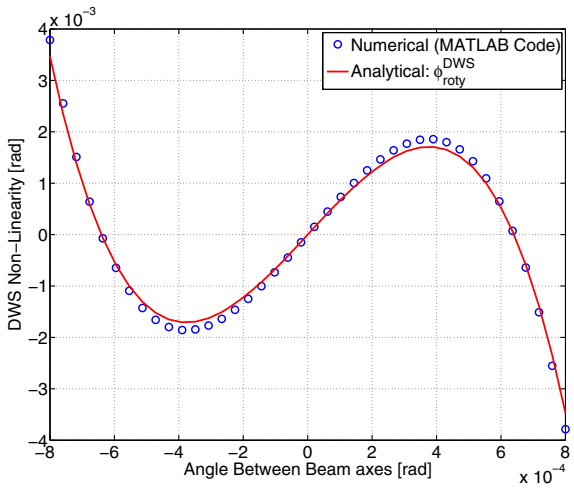

Fig. 3. DWS non-linearity calculated by numerical and theoretical method.

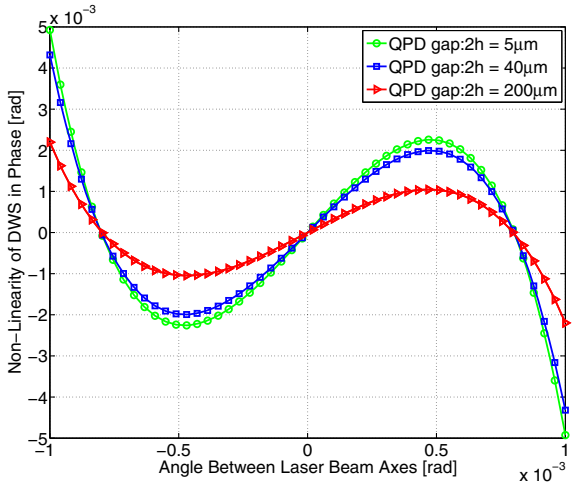

Fig. 4. DWS non-linearity for different QPD gaps (QPD edge is 1 mm).

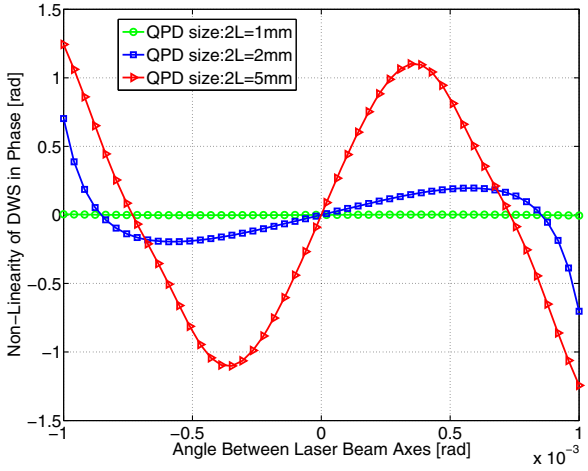

Fig. 5. DWS non-linearity for different QPD sizes (QPD gap is 5 μm).

different parameters, such as QPD gap and QPD size. The calculation results are shown in Figs. 4 and 5.

We set the beam waist radius of measurement and reference beams to be 1.9 mm. We calculated the non-linearity of DWS for different QPD gaps and sizes respectively. From Figs. 4 and 5, we can see that the DWS non-linearity increases with the increasing QPD size and decreasing QPD gap. That is to say, the beam clipping effect has a strong influence on the non-linearity of DWS detection. The reason why beam clipping affects DWS response is the inhomogeneous distribution of laser intensity. In other words, the phase signal we detected is the average phase weighted by the laser intensity distribution. Thus, intensity distribution will influence the detecting phase signals. Another important phenomenon in our system is the beam walking effect, which means the pivot of the laser beam does not locate in the detecting QPD surface. This is in line with the known property of the DWS signal to be insensitive to translations, but sensitive to the relative rotation between two laser wavefronts. Figure 6 shows the beam walking effect in

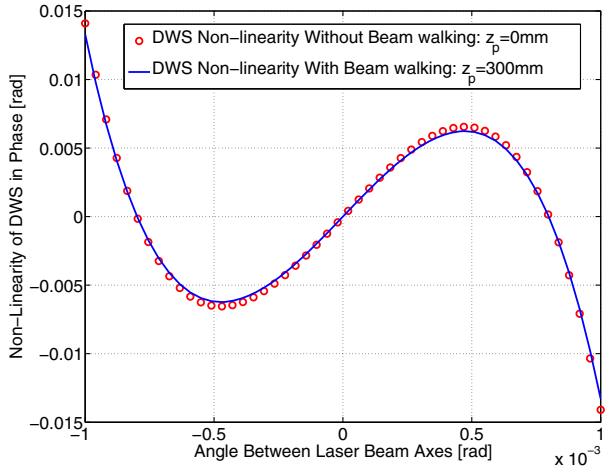

Fig. 6. DWS non-linearity with and without beam walking effect.

DWS detection. Calculation result shows that this effect hardly has any influence on DWS measurement.

We have built an analytical model for DWS measurement using a basic Gaussian beam model. The comparison between different analytical models and numerical methods indicates the high accuracy of our analytical expression. With this analytical expression, non-linearity of DWS has been studied. Results show that there is a milli-radians level of non-linearity in DWS detection. The non-linearity effect mainly comes from inhomogeneous distribution of the laser intensity, and it increases with increasing QPD size and decreasing QPD gap. Thus, the smaller beam clipping is, the stronger non-linearity is. From our analysis, the beam walking effect hardly has any influence on the non-linearity of DWS. DWS is a good choice for measurement of torsion pendulum rotation. If one measures the torsion pendulum rotation in 10 nrad accuracy, the non-linearity of 50 nrad is the limiting factor. The non-linearity must be calibrated and modified. In TianQin and LISA, the measurement accuracy for DWS is 10 nrad. If we consider the non-linearity in DWS, the performance of beam pointing control will be improved.

Funding. National Natural Science Foundation of China (NSFC) (91336109, 11405062, 11235004).

REFERENCES

1. B. S. Sheard, G. Heinzel, K. Danzmann, D. A. Shaddock, W. M. Klipstein, and W. M. Folkner, Journal of Geodynamics **86**, 1083 (2012).
2. G. D. Racca and P. W. McNamara, Space Sci. Rev. **151**, 159 (2010).
3. H. C. Yeh, Q. Z. Yan, Y. R. Liang, Y. Wang, and J. Luo, Rev. Sci. Instrum. **82**, 044501 (2011).
4. J. Luo, L. S. Chen, H. Z. Duan, Y. G. Gong, S. C. Hu, J. H. Ji, Q. Liu, J. W. Mei, M. Vadim, S. Mikhail, C. G. Shao, T. Viktor, H. B. Tu, Y. M. Wang, Y. Wang, H. C. Yeh, M. S. Zhan, Y. H. Zhang, Z. Vladimir, and Z. B. Zhou, Class. Quant. Grav. **33**, 035010 (2016).
5. G. Hechenblaikner, J. Opt. Soc. A **27**, 2078 (2010).
6. G. Wanner, G. Heinzel, E. Kochkina, C. Mahrdt, B. S. Sheard, S. Schuster, and K. Danzmann, Opt. Commun. **285**, 4831 (2012).
7. S. Schuster, G. Wanner, M. Tröbs, and G. Heinzel, Appl. Opt. **54**, 1010 (2015).
8. G. Wanner and G. Heinzel, Appl. Opt. **53**, 3043 (2014).
9. E. Kochkina, G. Wanner, D. Schmelzer, M. Tröbs, and G. Heinzel, Appl. Opt. **52**, 6030 (2013).